analytical chemistry

Article

pubs.acs.org/ac

Surface-Enhanced Raman Scattering Chip for Femtomolar Detection of Mercuric Ion (II) by Ligand Exchange

Yuanxin Du,[†] Renyong Liu,[‡] Bianhua Liu,[‡] Suhua Wang,[‡] Ming-Yong Han,[§] and Zhongping Zhang*[,†,‡]

[†]Department of Chemistry, University of Science & Technology of China, Hefei, Anhui 230026, China

[‡]Institute of Intelligent Machines, Chinese Academy of Sciences, Hefei, Anhui 230031, China

[§]Institute of Materials Research and Engineering, A-STAR, 3 Research Link, 117602, Singapore

Supporting Information

ABSTRACT: The chemical sensing for the convenient detection of mercuric ion (II) (Hg^{2+}) have been widely explored with the use of various sensing materials and techniques. It still remains a challenge to achieve ultrasensitive but simple, rapid, and inexpensive detection to metal ions. Here we report a surface-enhanced Raman scattering (SERS) chip for the femtomolar (fM) detection of Hg^{2+} by employing silver-coated gold nanoparticles (Au@Ag NPs) together with an organic ligand. 4,4′-Dipyridyl (Dpy) can control the aggregation of Au@Ag NPs via its dual interacting sites to Ag nanoshells to generate strong Raman hot spots and SERS readouts. However, the presence of Hg^{2+} can inhibit the aggregation of Au@Ag NPs by the coordination with Dpy, and as a result the SERS signals of Dpy are quenched. On the basis of these findings, a SERS chip has been fabricated by the assembly of Au@Ag NPs on a piece of silicon wafer and the further modification with Dpy. The exchange of Dpy from the chip into the aqueous Hg^{2+} droplet results in the quenching of Raman signals of Dpy, responding to 10 fM Hg^{2+} that is about 6 orders of magnitude lower than the limit defined by the U.S. Environmental Protection Agency in drinkable water. Each test using the SERS chip only needs a droplet of 20 μL sample and is accomplished within ~4 min. The SERS chip has also been applied to the quantification of Hg^{2+} in milk, juice, and lake water.

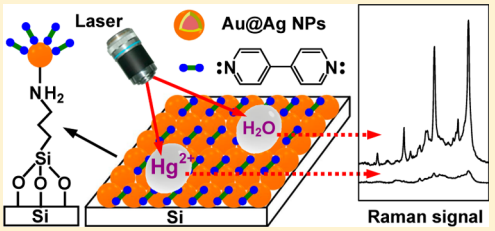

Heavy metal contamination in water, air, soil, or foods has remained a serious concern across the world for decades.[1] In particular, mercury, a very toxic element, can lead to a variety of permanent damages to human health even at a very low concentration,[2] and people are thus put on high alert to avoid the occurrence of shocking events, for example, the early mercury poisoning in Japan in 1956 and the recent Yili milk scandal in China in 2012. The maximum residue limit of mercuric ion (II) (Hg^{2+}) is 2 ppb (10 nM) in drinkable water as prescribed by the U.S. Environmental Protection Agency (EPA). The sensitive mercury assays are usually performed with a wealth of established techniques[3] including atomic absorption spectroscopy, inductively coupled plasma mass spectroscopy, anodic stripping voltammetry, X-ray fluorescence spectrometry, and neutron activation analysis. As these analyses are expensive, are time-consuming, and require tedious sample pretreatments and enrichments, and thus there is a great demand to develop a fast, sensitive, and reliable assay of Hg^{2+} residues for improving food safety and environmental protection.

Recently, considerable efforts have been devoted to explore such chemosensing approaches to the simple and on-site detection of Hg^{2+} via cooperative recognition and signaling by employing organic dyes or functionalized nanomaterials.[4−8] Different dye derivatives have been reported to selectively bind with Hg^{2+} for colorimetric and fluorescent assays,[4,5] and various nanomaterials such as plasmonic metal nanoparticles,[6] luminescent quantum dots[7] and conducting nanotubes[8] have also demonstrated to probe Hg^{2+} by the modification with ligands at their surfaces using the optical/electrical readout. Most of these methods can detect Hg^{2+} in the range of part-per-billion (ppb) to part-per-trillion (ppt). In order to decrease the detection limit to analyze the lower concentration of Hg^{2+} that may still do harm to our health after long-term accumulation, the more sensitive chemosensors to Hg^{2+} have been in the progress of exploration.

With the integration of high sensitivity, unique spectroscopic fingerprint, and nondestructive data acquisition, the surface-enhanced Raman scattering (SERS) technique has become one of the most widely pursued spectroscopic tools for the identification and detection of chemical and biological species.[9,10] The amplification of Raman signals is generally attributed to the electromagnetic (EM) field near the metal surface,[11] which leads to a 10^6−10^{15} enhancement factor dependent on the strength of EM experienced by the molecule at the surface of various metal nanostructures.[12] Different from organic/biological targets, however, metal ions including Hg^{2+} do not exhibit Raman signals, and thus their detection using the SERS technique can only be achieved by the indirect signal readout.[13−18] One of the most prevalent ways is to use DNA/oligonucleotides-conjugated dye tags to label the metal

Received: November 23, 2012
Accepted: February 25, 2013
Published: February 25, 2013

   dx.doi.org/10.1021/ac303358w | Anal. Chem. 2013, 85, 3160−3165

nanoparticles for the detection of Hg^{2+}.[13−15] Recently, some Raman-active ligands have been found to specifically interact with Hg^{2+}, inducing the aggregation of metal particles for the generation of the SERS effect.[16−18] These approaches either need the complex labeling procedure or only are performed in the solution system. Additionally, they have to suffer from unavoidable aggregation of metal nanoparticles by many environmental factors such as salts and organic molecules in samples, leading to the unambiguous problems for the determination of Hg^{2+} with false positives in real sample detections. The simultaneous achievements on the ultrasensitive, simple, rapid, and inexpensive advantages remain a crucial challenge to the metal ion sensors.

In the present study, we report a highly sensitive and selective SERS-based chemosensor for the femtomolar (fM) detection of Hg^{2+} in practical applications. The SERS chip was prepared via the assembly of silver-coated gold nanoparticles (Au@Ag NPs) onto a piece of silicon wafer followed by surface modification with 4,4′-dipyridyl (Dpy) to obtain strong SERS signal. Upon the addition of aqueous Hg^{2+} droplet, Dpy may exfoliate from the surface of Au@Ag NPs by strong coordination with Hg^{2+}, which leads to quenching the SERS signals of Dpy. The SERS chip can be used as a convenient indicator of Hg^{2+} residues at the femtomolar level with the use of only 20 μL sample, and the whole test can be accomplished within ∼4 min. The simple and rapid SERS-based chip sensor reported here exhibits high sensitivity and reliability in the assay of real samples and thus opens a novel avenue to fabricate SERS-based sensors.

EXPERIMENTAL SECTION

Chemicals and Materials. 4,4′-Dipyridyl (Dpy), pyridine, 2,2-bipyridine, benzidine, sodium citrate ($Na_3C_6H_5O_7·2H_2O$, 99.8%), chloroauric acid ($HAuCl_4·4H_2O$, 99.9%), silver nitrate ($AgNO_3$, 99%), ascorbic acid (99%), hydrogen peroxide (H_2O_2, 30%), sulfuric acid (H_2SO_4, 98%), nitric acid (HNO_3, 65%), ammonia solution, ethanol, acetone, $Hg(NO_3)_2$, $FeCl_3·6H_2O$, $CuCl_2$, $CdCl_2·2.5H_2O$, $CoCl_2·6H_2O$, $NiCl_2·6H_2O$, $Pb(NO_3)_2$, $ZnCl_2$, $MgCl_2·6H_2O$, $MnSO_4·H_2O$, NaCl, and $LiCl·H_2O$ were purchased from Sinopharm Chemical Reagent Co., Ltd. (Shanghai, China). 3-Aminopropyltriethoxysilane (3-APTS) was obtained from Sigma-Aldrich. 2,2′:6′,2″-Terpyridine (98%) was supplied from Aladdin. All of these reagents were used without further purification. Ultrapure water (18.2 MΩ cm) was produced using a Millipore water purification system. The real lake water was collected from a local lake, and the milk and fruit juice used in this research were directly purchased from a local supermarket.

Synthesis of Au and Ag NPs with 30-nm Size. Typically, 0.25 mL of 0.1 M $HAuCl_4$ was added into 100 mL of ultrapure water and then heated to boiling under magnetic stirring. After quickly injecting 1.5 mL of 1% trisodium citrate, the mixed solution was refluxed for ∼30 min until it became wine red. After gradually cooling to room temperature under stirring, the resulting solution was filtered through a 0.22 μm Millipore membrane, and the Au NPs colloid with the size of 30 nm was stored in a refrigerator at 4 °C for further use. Meanwhile, Ag NPs of 30-nm size were also synthesized. Briefly, 90 mg of silver nitrate was dissolved in 250 mL of ultrapure water and brought to boiling. To this solution, 10 mL of 1% trisodium citrate was added and kept boiling for 1 h. After cooling to room temperature, the Ag NPs colloid was obtained.[19] The Au and Ag NPs concentrations are ∼0.24 and 0.60 nM, respectively, which are calculated using Beer's law and the extinction coefficients (ε) (30-nm Au and Ag NPs are 3.0×10^9 and 2.3×10^{10} M^{-1} cm^{-1}, respectively).

Synthesis of Au@Ag NPs. Typically, 10 mL of the above Au NPs colloid and 1.5 mL of 0.1 M ascorbic acid were mixed in a round flask under magnetic stirring. Then 3.5 mL of 1 mM $AgNO_3$ was dropwise added into the above mixture at a rate of one drop per 30 s. Silver nitrate was reduced by ascorbic acid and the resultant silver continuously grew at the surface of Au seeds. After the wine red of solution changed into orange, the solution was stirred for 30 min and the Au@Ag NPs were obtained.[20] According to the initial concentration of Au cores and the change of volume, the final concentration of Au@Ag NPs is estimated to be ∼0.16 nM based on the assumption that silver ions are completely reduced on Au cores.

Raman Detections of Hg^{2+} in Water. Briefly, different concentrations of Hg^{2+} were first mixed well with the Dpy solution (1.0×10^{-5} M) in 100 μL of ultrapure water for 5 min, and then the mixed solution was added into the Au@Ag NPs monodispersion (900 μL) in a 1.5-mL centrifuge tube, followed by shaking for 1 min. The mixture was first sucked into a capillary glass tube, which was then fixed onto a glass slide. The Raman spectra were recorded using a 532-nm laser with 10 mW power and 10× objective (2.1-μm^2 spot). The integral time is 2 s with 2 rounds of accumulations, and the slit aperture is 50 μm. The experiments were replicated five times for each concentration. Other metal ions were also detected using the same method.

Raman Measurements of Hg^{2+} in Real Samples. The SERS chip for ultrasensitive detection of Hg^{2+} was fabricated by the assembly of Au@Ag NPs on a piece of silicon wafer and the further modification with Dpy. First, a silicon wafer was cleaned by sequential ultrasonication in acetone, ethanol, ultrapure water for 15 min in each, then treated with H_2SO_4/H_2O_2 (3:1 v/v) at 80 °C for 30 min and then ultrasonication in ultrapure water/ammonia solution/H_2O_2 (5:1:1 v/v/v) for 30 min to derive a hydroxyl surface. After thorough rinsing with ultrapure water and ethanol, the cleaned silicon wafer was dried in the air. Second, the clean silicon wafer was immersed into 10% APTS ethanol solution for 16 h to form the monolayer of APTS with an $-NH_2$ end group. The wafer was then rinsed profusely with ethanol to remove unbound monomer from the surface and dried in air. Third, the APTS-modified silicon wafer was submerged into colloidal Au@Ag NPs for 6 h, resulting in the formation of a layer of Au@Ag NPs on the silicon surface.[21] Finally, the silicon wafer was further immersed into 1.0×10^{-5} M of Dpy solution for 4 h at room temperature to obtain a SERS chip for the selective detection of Hg^{2+}.

A volume of 2 mL of Hg^{2+} solution with different concentrations was spiked into 2 mL of lake water, commercial fruit juice, and milk followed by the addition of 4 mL of 65% HNO_3. The mixture was incubated at 95 °C for 2 h and cooled to room temperature, and the pH of the solution was adjusted to 7.0. After centrifugation, the clear supernatant was collected and filtered through 0.45 μm Supor filters to remove any particulate suspension. Prior to the assay, the samples were diluted 100 times with ultrapure water so that the level of Hg^{2+} was within the linear range. Then, 20 μL of sample solution was evenly dropped onto the modified SERS chip. The time-resolved Raman spectra were immediately recorded with 532-nm laser with 5-mW power and 50× objectives (1-μm^2 spot). The integral time is 10 s, and the slit aperture is 50 μm. The

dx.doi.org/10.1021/ac303358w | Anal. Chem. 2013, 85, 3160−3165

interval period for the collection of the Raman spectra was set at 20 s.

Characterization and Instruments. The prepared Au@Ag NPs were characterized by field-emission scanning microscopy (FE-SEM, Sirion 200) and transmission electron microscopy (TEM, JEOL 2010), respectively. UV−vis absorption spectra were recorded with a Shimadzu UV-2550 spectrometer. Raman measurements were conducted with a Thermo Fisher DXR Raman microscope equipped with a CCD detector.

RESULTS AND DISCUSSION

Figure 1 illustrates the SERS sensing mechanism for detection of Hg^{2+} by employing core−shell Au@Ag NPs together with

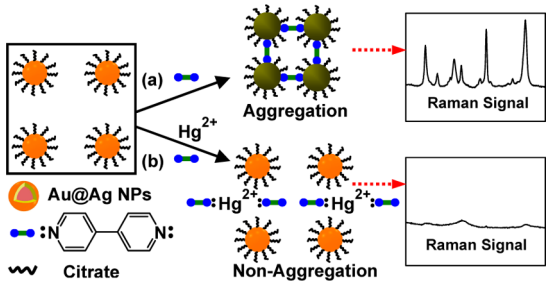

Figure 1. Schematic illustration of the interaction between Au@Ag NPs and 4,4′ -dipyridyl (Dpy) in (a) the absence and (b) the presence of Hg^{2+}, and the corresponding SERS responses.

organic ligand 4,4′-dipyridyl (Dpy). The Au@Ag NPs were prepared by seeded growth through a consecutive two-step process (see details of the synthesis procedure in the Experimental Section).[20] The as-synthesized Au@Ag NPs have an average size of ∼45 nm, and the thickness of their silver shells is ∼7 nm (see the SEM and TEM images of Figure S1 in the Supporting Information). With the wider plasmon resonance range, Au@Ag NPs exhibit a better SERS effect than pure Au and Ag NPs[22] and have been used as SERS particle sensors for the detection of pesticide residues at various peels of fruits, as reported earlier.[20] Also, it is known that the silver shell of Au@Ag NPs can adsorb organic ligands with electron-rich structures. With an electronic-rich structure, Dpy molecules can be adsorbed on the silver shell of Au@Ag NPs. As each Dpy molecule has two pyridine rings in a symmetrical form, the two electron-rich nitrogen atoms can bind to the silver shells of two Au@Ag NPs.[4,23] As drawn in Figure 1a, the aggregation will quickly occur upon the addition of Dpy into Au@Ag NPs colloid, leading to a strong Raman hot spot effect and SERS readouts. On the other hand, the two electron-rich nitrogen atoms at the Dpy molecule are highly specific to Hg^{2+} by an effective coordinative reaction,[4,24] which is much stronger than to other metal ions (see hereinafter text). When Dpy was first mixed with Hg^{2+} to form the Hg^{2+}-Dpy complex and then added into the colloidal solution, the aggregation did not occur. That is to say, Hg^{2+} has a very strong coordination ability to Dpy, which obviously exceeds the binding ability between Dpy and Ag nanoshells. As a result, the Au@Ag NPs still keep a monodispersive state after the addition of mixing Hg^{2+} and Dpy solution. The strong Raman signal of Dpy cannot be detected at all due to the lack of a Raman hot spot and SERS effect (Figure 1b). Therefore, Hg^{2+} can quench the Raman signals of Dpy in Au@Ag NPs colloid to provide an ultrasensitive detection of Hg^{2+}.

The above concept for the detection of Hg^{2+} has been further evidenced by the UV−vis spectroscopy characterizations and TEM examinations. The original Au@Ag NPs is displayed as bright orange and had a wide range of plasmon resonance absorption from 320 to 560 nm, resulting from the overlapping and interaction of two different plasmon resonance frequencies of Ag nanoshells and Au cores in the core−shell nanoparticles (the blank line in Figure 2A). Meanwhile, the UV−vis

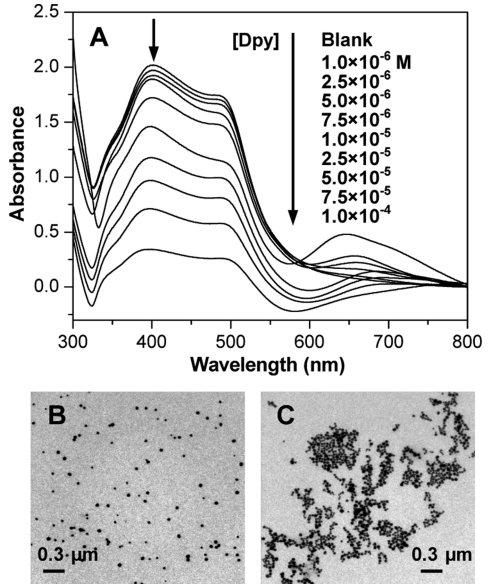

Figure 2. (A) UV−vis absorption spectra of Au@Ag NPs colloid with the increase of Dpy concentration. The TEM images of Au@Ag NPs states (B) in the absence and (C) in the presence of 1.0×10^{-4} M Dpy.

spectroscopy (Figure 2A) revealed that with the increase of Dpy concentration from 1.0×10^{-6} to 1.0×10^{-4} M in the colloid, the absorbance of Au@Ag NPs decreased gradually and a new absorbance centered at 650 nm appeared. These results indicate that Dpy can obviously induce the aggregation of Au@Ag NPs. This was further confirmed by the TEM observations: the monodisperse Au@Ag NPs in the absence of Dpy and the significant aggregation of Au@Ag NPs in the presence of 1.0×10^{-4} M Dpy (parts B and C of Figure 2, respectively). As shown in Figure 1, the Dpy molecule has two pyridine rings to bind Ag shells and thus plays a role of cross-linking agent to effectively induce the occurrence of colloidal aggregation.

Figure 3A shows the optical photos of Au@Ag colloid color change and the SERS spectra of Dpy in the colloidal Au@Ag NPs. Upon the addition of Dpy into the colloid, the color of Au@Ag NPs changed from orange to deep green which indicates Au@Ag NPs gradually aggregated. Meanwhile, the Raman signals of Dpy became significantly stronger. Even at the concentration of 1.0×10^{-6} M, the typical Raman peaks of Dpy including 786, 1016, 1078, 1296, and 1614 cm^{-1} can be clearly detected (see the assignments of peaks in Table S1 in the Supporting Information), which implies the formation of hot spots at the junction of aggregating particles (as illustrated in Figure 1a). Although the similar behaviors also occurred in the pure Ag and Au NPs colloid, the enhancement effect of Au@Ag NPs was ∼20- and 10-fold those of pure Au and Ag NPs, respectively (see Figure S2 in the Supporting Information). The better enhanced effect may result from the

dx.doi.org/10.1021/ac303358w | Anal. Chem. 2013, 85, 3160−3165

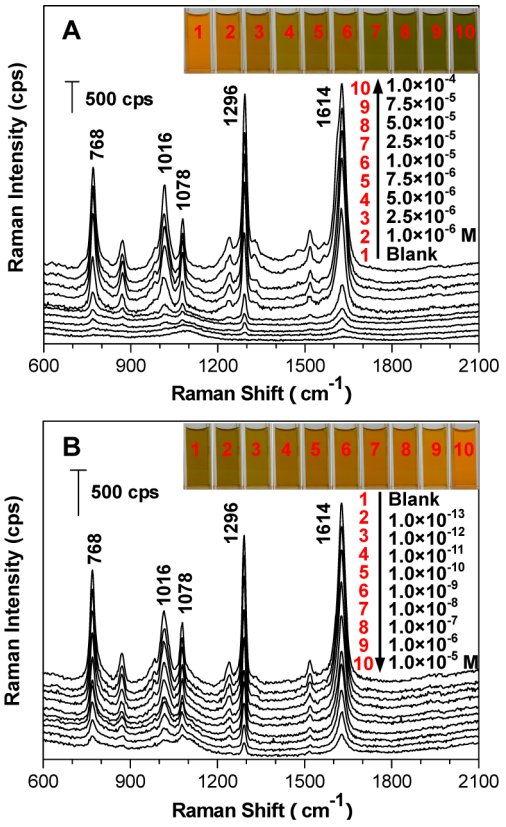

Figure 3. (A) SERS spectra of Dpy in colloidal Au@Ag NPs with the increase of Dpy amounts (the inset is the corresponding color images). (B) Evolution of SERS spectra of Dpy (1.0×10^{-5} M) in colloidal Au@Ag NPs with the increase of Hg^{2+} concentration from 1.0×10^{-13} to 1.0×10^{-5} M (the inset is the corresponding color images).

coupling of plasmon resonance of Ag nanoshells and Au cores.[20,25]

However, it is interesting that the coexistence of Hg^{2+} and Dpy can obviously inhibit the particle aggregation. Here, the effect of Hg^{2+} concentration on the SERS intensity was investigated under the constant concentration of Dpy at 1.0×10^{-5} M. As shown in the image of Figure 3B, the increase of Hg^{2+} in the system led to the change of color from green to orange. Meanwhile, the optical absorbance gradually recovered and the absorption peak at ~650 nm originating from the Au@Ag aggregates decreased systematically (Figure S3 in the Supporting Information). When the concentration of Hg^{2+} increased to 1.0×10^{-6} M, the absorption was almost recovered to that of bare Au@Ag NPs. These confirm that the extremely strong coordination ability of Hg^{2+} with Dpy leads to the formation of the Hg^{2+}-Dpy complex and the aggregation of Au@Ag NPs will not occur. Because of the lack of hot spots, the Raman signals of Dpy in this system gradually decreased with the increase of Hg^{2+} concentration from 1.0×10^{-13} to 1.0×10^{-5} M (Figure 3B). Even at the concentration of 1.0×10^{-13} M Hg^{2+}, the intensity of the strongest peak at 1614 cm^{-1} decreased about 5%, revealing the high sensitivity of this SERS system to Hg^{2+}.

In order to confirm the above mechanism, other structural-like amino compounds with electron-rich functional groups, including benzidine, 2,2-bipyridine, pyridine, and 2,2′:6′,2″-terpyridine were also used as SERS active ligands to evaluate the sensitivity of Dpy to Hg^{2+}. Figure S4 in the Supporting Information shows the individual SERS spectra of the five compounds, and their strongest peaks at 1614, 1606, 1489, 1007, and 1554 cm^{-1} were used for quantitative detection of Hg^{2+}, respectively. At the concentration of 1.0×10^{-7} M Hg^{2+}, the quenching percentages of the Raman intensity was ~84% for Dpy, ~52% for benzidine, ~18% for 2,2-bipyridine, ~8% for pyridine, ~4% for 2,2′:6′,2″-terpyridine. These results confirm that the higher spectra selectivity of Dpy to Hg^{2+} because of the stronger coordinative ability of Hg^{2+} with Dpy than with other ligands. Furthermore, the specificity of this system to Hg^{2+} was tested by the SERS response upon the addition of other metal ions with concentrations of 1.0×10^{-6} M. The metal ions such as Co^{2+}, Cu^{2+}, Fe^{3+}, Li^{+}, Mn^{2+}, Mg^{2+}, Na^{+}, Cd^{2+}, Pb^{2+}, and Zn^{2+} did not almost exhibit the quenching effect to the SERS signals of Dpy (Figure S5 in the Supporting Information) due to the low binding affinity of Dpy to them.[4] These above observations reveal the high selectivity of this SERS system to Hg^{2+} by the use of Dpy.

On the basis of the above concept, a SERS chip for the convenient detection of Hg^{2+} has been fabricated by the assembly of Au@Ag NPs on a piece of silicon wafer and the further modification with Dpy at the concentration of 1.0×10^{-5} M (see the details in the Experimental Section). 3-Aminopropyltriethoxysilane (3-APTS) was first linked onto the surface of the chemically treated silicon wafer to form the monolayer of APTS with the $-NH_2$ end group,[26] as shown in Figure 4A. When the wafer was immersed into the Au@Ag NPs colloid, the Au@Ag NPs automatically adsorbed onto the surface of the wafer by the interaction between the particles and the $-NH_2$ end groups, resulting in a dense/stable monolayer of

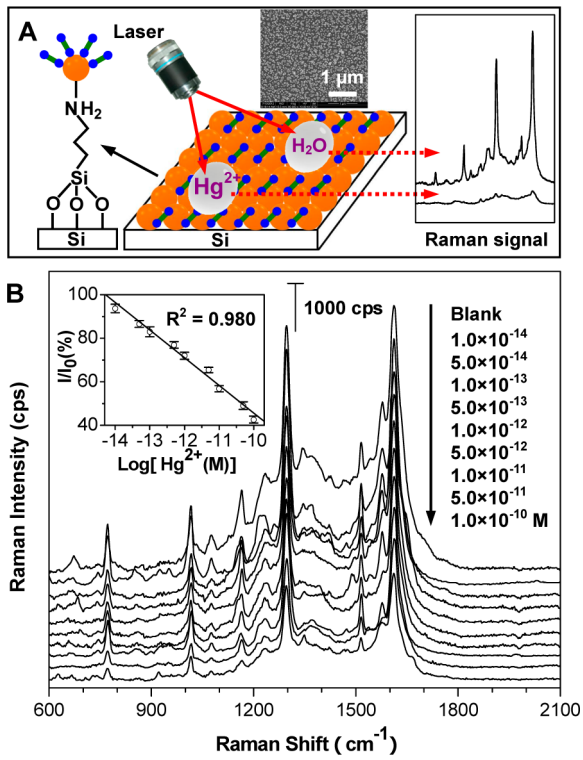

Figure 4. (A) Schematic drawing for direct detection of Hg^{2+} with the SERS chip fabricated by the assembly of Au@Ag NPs on a silicon wafer. (B) Evolution of SERS spectra of Dpy with the addition of an aqueous Hg^{2+} droplet. The inset is the linear correlation of Raman intensity (at 1614 cm^{-1}) with the logarithm of Hg^{2+} concentrations from 1.0×10^{-14} to 1.0×10^{-10} M.

dx.doi.org/10.1021/ac303358w | Anal. Chem. 2013, 85, 3160−3165

Au@Ag NPs on the substrate (the SEM image of Figure 4A). Subsequently, the SERS chip was further modified with Dpy in solution to obtain strong and uniform Raman readouts of Dpy (Figure S6 in the Supporting Information). Importantly, when a droplet of 20 μL of pure water was added onto this chip, the Raman intensity focused on the droplet kept was unchangeable (Figure S7 in the Supporting Information), indicating the stable adsorption of Dpy at the monolayer of Au@Ag NPs. On the contrary, the Raman signals of Dpy obviously quenched if the same water droplet containing Hg^{2+} was added onto the chip, which is attributable to the exfoliation of Dpy ligands from the monolayer of Au@Ag NPs into the liquid droplet by the formation of Hg^{2+}-Dpy complex. The quenching degree reached the maximum and was kept stable after ~4 min (Figure S7 in the Supporting Information). Therefore, the SERS chip can be used for the fast detection of trace Hg^{2+} with a very little amount of sample.

Figure 4B shows the Raman test results by adding a droplet of 20 μL of water containing different concentrations of Hg^{2+}. With the increase in the concentration of Hg^{2+} from 1.0×10^{-14} to 1.0×10^{-10} M, the Raman intensity of Dpy dramatically decreased. The intensity of the strongest peak at 1614 cm^{-1} was used for the quantitative evaluation of the Hg^{2+} level and exhibited a good linear relationship with the concentration ranging from 1.0×10^{-14} to 1.0×10^{-10} M ($R^2 = 0.980$). The limit of detection was determined to be 1.0×10^{-14} M from three standard deviations above the background, which is about 6 orders of magnitude lower than the U.S. EPA defined limit in drinkable water. The excellent specificity of the SERS chip to Hg^{2+} was also demonstrated by the test of other metal ions with concentrations of 1.0×10^{-6} M (Figure 5A). Furthermore, it is noted that the SERS chip can be cyclically used by remodification with Dpy (Figure 5B).

In order to verify the usefulness of the proposed sensor for the identification and detection of Hg^{2+} in practical applications, the detection of natural Hg^{2+} in real samples (milk, orange juice, and lake water) was demonstrated here by the use of the SERS chip (Figure S8 in the Supporting Information). The samples only need to be pretreated by simple incubation and centrifugation (see the Experimental Section). Prior to the assay, the samples were diluted 100 times with ultrapure water so that the level of Hg^{2+} was within the linear ranges. The data listed in Table 1 indicated that the obtained results were highly consistent with those from the atomic fluorescence spectrometry (AFS) method. Meanwhile, when the known amount of Hg^{2+} was added in these samples, the recovery of Hg^{2+} ranged from 98.33% to 107.77%. These confirm that the SERS chip has a high accuracy, reliability, and sensitivity to meet the requirements of the application.

CONCLUSIONS

In summary, ultrasensitive detection of Hg^{2+} mainly comes from the use of highly SERS-active nanoparticles, the choice of appropriate organic ligands, and the formulation of the excellent working conditions. The three factors work collectively on the SERS chip: (1) metal nanoparticles can adsorb the organic ligand to exhibit a strong SERS effect; (2) the highly SERS-active ligand has selective coordination ability to target ions; and (3) the addition of analyte can exfoliate the adsorbed ligand from the nanoparticle substrate by analyte to quench the SERS signals. We have successfully fabricated the SERS chip by assembling core–shell Au@Ag NPs to achieve an ultrahigh sensitivity to Hg^{2+} down to the femtomolar level,

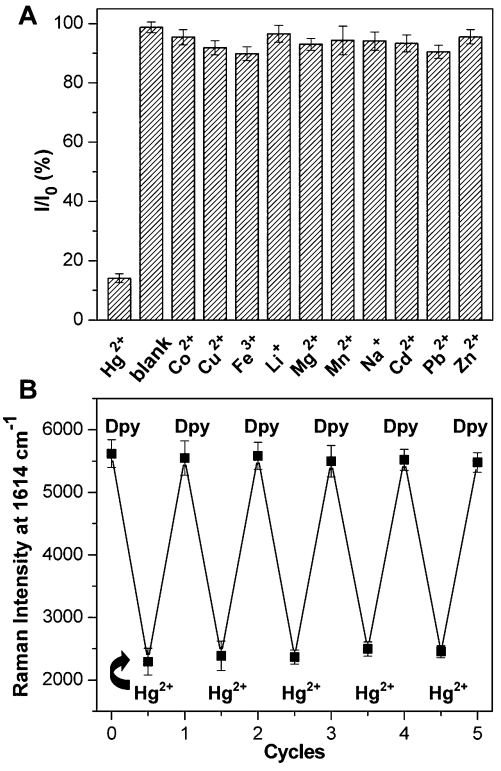

Figure 5. (A) Selectivity of the SERS chip for the detection of Hg^{2+} over other metal ions. The SERS intensity of the peak at 1614 cm^{-1} was used for the evaluation of the Raman readout. (B) Cyclic detection of Dpy Raman intensity at 1614 cm^{-1} by repeatedly adding 20 μL of 1.0×10^{-10} M Hg^{2+} solution onto the assembled SERS chip and modifying with 1.0×10^{-5} M Dpy.

Table 1. Real Detection and Recovery Test of Hg^{2+} in Different Samples

sample	AFS method (pmol/L)[a]	proposed SERS method (pmol/L)[b]	spiked Hg^{2+} (pmol/L)	measured Hg^{2+} (pmol/L)	recovery (%)
milk	11.20	0.11	0.50	0.60	98.36
orange juice	9.96	0.10	0.50	0.59	98.33
lake water	54.80	0.53	0.50	1.11	107.77

[a]The data represent natural Hg^{2+} levels detected by standard atomic fluorescence spectrometry. [b]The Hg^{2+} concentrations were obtained after 100 times dilution with ultrapure water.

which greatly exceeds the previously reported results. This SERS chips possess many advantages, such as excellent anti-interference ability, recycling usage, long-term stability, portable feasibility, and simple operation. This technique is very simple and inexpensive as compared to early methods, and each test only needs a very little amount of sample. This SERS-chip technique may be extended to open a novel avenue to develop various SERS-based sensors.

ASSOCIATED CONTENT

Supporting Information

UV–vis absorption spectra; SERS spectra of Dpy, benzidine, 2,2-bipyridine, pyridine, and 2,2′:6′,2″-terpyridine; and SERS detection of Dpy in milk, orange juice, and lake water. This material is available free of charge via the Internet at http://pubs.acs.org.

dx.doi.org/10.1021/ac303358w | Anal. Chem. 2013, 85, 3160–3165

AUTHOR INFORMATION

Corresponding Author

*E-mail: zpzhang@iim.ac.cn.

Notes

The authors declare no competing financial interest.

ACKNOWLEDGMENTS

Thank for the supports from National Key Technology R&D Program (Grant 2012BAJ24B02) and the Natural Science Foundation of China (Grant Nos. 61205152, 21175137, 21077108, and 20925518).

REFERENCES

(1) Nriagu, J. O. *Nature* **1979**, *279*, 409−411.
(2) Nolan, E. M.; Lippard, S. J. *Chem. Rev.* **2008**, *108*, 3443−3480.
(3) Clevenger, W. L.; Smith, B. W.; Winefordner, J. D. *Crit. Rev. Anal. Chem.* **1997**, *27*, l−26.
(4) Li, Y.; Wu, P.; Xu, H.; Zhang, Z. P.; Zhong, X. H. *Talanta* **2011**, *84*, 508−512.
(5) Yang, Y. K.; Yook, K. J.; Tae, J. S. *J. Am. Chem. Soc.* **2005**, *127*, 16760−16761.
(6) Lee, J. S.; Han, M. S.; Mirkin, C. A. *Angew. Chem., Int. Ed.* **2007**, *46*, 4093−4096.
(7) Freeman, R.; Finder, T.; Willner, I. *Angew. Chem., Int. Ed.* **2009**, *48*, 7818−7821.
(8) Khani, H.; Rofouei, M. K.; Arab, P.; Gupta, V. K.; Vafaei, Z. *J. Hazard. Mater.* **2010**, *183*, 402−409.
(9) Smith, W. E. *Chem. Soc. Rev.* **2008**, *37*, 955−964.
(10) Liu, R. Y.; Liu, B. H.; Guan, G. J.; Jiang, C. L.; Zhang, Z. P. *Chem. Commun.* **2012**, *48*, 9421−9423.
(11) Jeanmaire, D. L.; Van Duyne, R. P. *J. Electroanal. Chem.* **1977**, *84*, 1−20.
(12) Pieczonka, N. P. W; Aroca, R. F. *Chem. Soc. Rev.* **2008**, *37*, 946−954.
(13) Kang, T.; Yoo, S. M.; Kang, M.; Lee, H.; Kim, H.; Lee, S. Y.; Kim, B. *Lab Chip* **2012**, *12*, 3077−3081.
(14) Han, D.; Lim, S. Y.; Kim, B. J.; Piao, L.; Chung, T. D. *Chem. Commun.* **2010**, *46*, 5587−5589.
(15) Kang, T.; Yoo, S. M.; Yoon, I.; Lee, S.; Choo, J.; Lee, S. Y.; Kim, B. *Chem.—Eur. J.* **2011**, *17*, 2211−2214.
(16) Duan, J.; Yang, M.; Lai, Y. C.; Yuan, J. P.; Zhan, J. H. *Anal. Chim. Acta* **2012**, *723*, 88−93.
(17) Li, F.; Wang, J.; Lai, Y. M.; Wu, C.; Sun, S. Q.; He, Y. H.; Ma, H. *Biosens. Bioelectron.* **2013**, *39*, 82−87.
(18) Grasseschi, D.; Zamarion, V. M.; Araki, K.; Toma, H. E. *Anal. Chem.* **2010**, *82*, 9146−9149.
(19) Kanjanawarut, R.; Su, X. D. *Anal. Chem.* **2009**, *81*, 6122−6129.
(20) Liu, B. H.; Han, G. M.; Zhang, Z. P.; Liu, R. Y.; Jiang, C. L.; Wang, S. H.; Han, M. Y. *Anal. Chem.* **2012**, *84*, 255−261.
(21) Liu, X. J.; Cao, L. Y.; Song, W.; Ai, K. L.; Lu, L. H. *ACS Appl. Mater. Interfaces* **2011**, *3*, 2944−2952.
(22) Rycenga, M.; Cobley, C. M.; Zeng, J.; Li, W. Y.; Moran, C. H.; Zhang, Q.; Dong, Q.; Xia, Y. N. *Chem. Rev.* **2011**, *111*, 3669−3712.
(23) Braun, G.; Pavel, I.; Morrill, A. R.; Seferos, D. S.; Bazan, G. C.; Reich, N. O.; Moskovits, M. *J. Am. Chem. Soc.* **2007**, *129*, 7760−7761.
(24) Xie, Y. M.; Wu, J. H. *Acta Crystallogr., C* **2007**, *63*, m220−m222.
(25) Pena-Rodríguez, O.; Pal, U. *Nanoscale* **2011**, *3*, 3609−3612.
(26) Gao, D. M.; Wang, Z. Y.; Liu, B. H.; Ni, L.; Wu, M. H.; Zhang, Z. P. *Anal. Chem.* **2008**, *80*, 8545−8553.